

Signature of large-gap quantum spin Hall state in the layered mineral jacutingaite

Konrád Kandrai¹, Péter Vancsó¹, Gergő Kukucska², János Koltai², György Baranka¹, Ákos Hoffmann¹, Áron Pekker³, Katalin Kamarás³, Zsolt E. Horváth¹, Anna Vymazalová⁴, Levente Tapasztó¹, and Péter Nemes-Incze^{1, †}

¹Centre for Energy Research, Institute of Technical Physics and Materials Science, 1121 Budapest, Hungary

²ELTE Eötvös Loránd University, Department of Biological Physics, 1117 Budapest, Hungary

³Wigner Research Centre for Physics, Institute for Solid State Physics and Optics, 1121 Budapest, Hungary

⁴Czech Geological Survey, 152 00 Prague, Czech Republic

[†]*corresponding author, email: nemes@mfa.kfki.hu*

June 22, 2020

Abstract

Quantum spin Hall (QSH) insulators host edge states, where the helical locking of spin and momentum suppresses backscattering of charge carriers, promising applications from low-power electronics to quantum computing. A major challenge for applications is the identification of large gap QSH materials, which would enable room temperature dissipationless transport in their edge states. Here we show that the layered mineral jacutingaite (Pt_2HgSe_3) is a candidate QSH material, realizing the long sought-after Kane-Mele insulator. Using scanning tunneling microscopy, we measure a band gap in excess of 100 meV and identify the hallmark edge states. By calculating the \mathbb{Z}_2 invariant, we confirm the topological nature of the gap. Jacutingaite is stable in air and we demonstrate exfoliation down to at least two layers and show that it can be integrated into heterostructures with other two-dimensional materials. This adds a topological insulator to the 2D quantum material library.

Keywords: Topological insulator, Low-dimensional materials, Quantum spin Hall effect (QSH), Scanning tunneling microscopy (STM)

The QSH state^{1;2} has first been realized experimentally, at cryogenic temperatures, in HgTe quantum wells³. Interestingly, the prototype QSH insulator is actually graphene, when it was realized by Kane and Mele that its Dirac quasiparticles are gapped and characterized by a \mathbb{Z}_2 topological invariant if spin orbit coupling (SOC) is considered^{4;5}. However, the low SOC in graphene results in a gap of only a few μeV , making its topological properties a mere theoretical curiosity. To realize a Kane-Mele insulator, a material is needed with the honeycomb lattice of graphene, but having large SOC⁴. In the last few years there has been a tremendous effort to find a layered material conforming to these requirements. From the point of view of applications, the candidate material forming this "heavy metal graphene", should ideally have the following characteristics. It should have a topological gap above room temperature, to enable room temperature dissipationless charge transport. The van der Waals bonding between the layers of the material should be weak enough⁶ to enable exfoliation

by the well known methods developed for 2D materials. This would enable integration into heterostructures with the vast numbers of other 2D quantum materials discovered to date^{7;8}. Such a combination with other 2D materials can enable a high degree of control over the edge states⁷. For example, in proximity with 2D superconductors, Majorana quasiparticles could be formed⁹. Lastly, it should be stable in air under ambient conditions, making the material widely usable.

One possibility to realize a QSH system, is to increase the SOC in graphene by placing it in proximity to materials with a large atomic number^{10–12}, either using adatoms^{13;14} or in a substrate^{15–17}. The resulting SOC induced gap is of the order of 10 meV at best. An alternative is to find a material with an intrinsically large topological gap¹⁸, such as a bismuth honeycomb layer on SiC^{19;20}, with a band gap of 0.8 eV. However, the crystal structure and therefore the topological properties of this bismuthene are linked to the SiC support, limiting its applicability. Similar constraints arise in the case of stanene²¹ and other group IV honeycomb layers and perhaps for bismuth (111) bilayers^{22;23}.

Among materials that exist as freestanding single layers, the 1T' phase of transition metal dichalcogenides are predicted to be QSH insulators²⁴. For MoS₂, WSe₂ and WTe₂ the hallmark edge states have been identified by scanning tunneling microscopy (STM)^{25–29} and by charge transport measurements for WTe₂³⁰. However, MoS₂ and WSe₂ are metastable and easily convert to the 2H phase³¹, while WTe₂ is stable in the 1T' polymorph, but rapidly oxidizes in air. None of the above examples are stable under ambient conditions, with the possible exception of Bi₁₄Rh₃I₉³². However, due to the complex crystal structure and ionic bonding between the layers³³, it is not clear if it is possible to isolate a single layer of it.

Here we present evidence via STM measurements that jacutingaite (Pt₂HgSe₃), a naturally occurring mineral^{34;35}, realizes a room temperature Kane-Mele insulator, satisfying all of the above criteria. By measuring on the basal plane of exfoliated multilayer crystals, we identify a bulk band gap and edge states within this gap, localized to monolayer step edges, showing a decay length of 5 Å into the bulk. We reproduce the measured band gap and edge states by density functional theory calculations (DFT) of the monolayer. By calculating the \mathbb{Z}_2 invariant, we show that the band gap is expected to be topologically non-trivial, in accordance with the previous

prediction of Marrazzo et al.³⁶. Within our experiments Pt_2HgSe_3 has proven to be stable under ambient conditions, on a timescale of months to a year, either as bulk or exfoliated crystals with a thickness down to 1.3 nm, equivalent to one or two layers. This is no surprise since jacutingaite is a mineral^{34;35}, therefore it should be stable not just under ambient but at pressures and temperatures relevant to geological processes.

The sample we investigated was grown synthetically, as described previously³⁵. For preparation and characterization details, see Supplementary section S1. Additionally, we have measured and calculated the Raman spectrum of bulk crystals, see Supplement S6. In the following, we focus on STM measurements of exfoliated thick crystals on a gold surface. The measurements were carried out in UHV at a base pressure of 5×10^{-11} Torr and a temperature of 9 K.

Jacutingaite is a ternary compound having a "sandwich-like" structure reminiscent of transition metal dichalcogenides, with a platinum layer between selenium and mercury. It can be regarded as "heavy metal graphene", since states around the SOC induced gap are localized on the honeycomb lattice formed by Pt and Hg atoms (see bottom inset in Fig. 1a)³⁶. Indeed, in the absence of SOC these bands give rise to a Dirac cone at the K points of the Brillouin zone (see Fig. 1b).

The atomic resolution STM images of the basal plane reflect this honeycomb structure, for an example see Fig. 1a. The topographic image shows a sublattice symmetry broken graphene-like arrangement of the local density of states (LDOS), with the unit cell shown by a red rhombus. The unit cell size is measured to be 7.3 Å, in agreement with the expected unit cell size (7.34 Å) measured via X-ray diffraction³⁵. Upon closer examination, we can observe a difference in the apparent height of the two sublattices, marked by red squares and triangles in Fig. 1a. This sublattice symmetry breaking is a consequence of the buckled honeycomb nature of the Pt-Hg lattice. The buckling means that each inequivalent sublattice resides on opposing sides of the single layer, similarly to silicene or germanene.

Measuring the differential tunneling conductivity ($dI/dV(V)$) on the defect free basal plane, reveals a bulk band gap of 110 mV, shown by the gray shading in Fig. 1c. Importantly, if measured far away from any surface defects or edges, the dI/dV signal goes to zero inside the gap, showing that this energy range is indeed devoid of electronic states. The measured LDOS is in excellent agreement with density

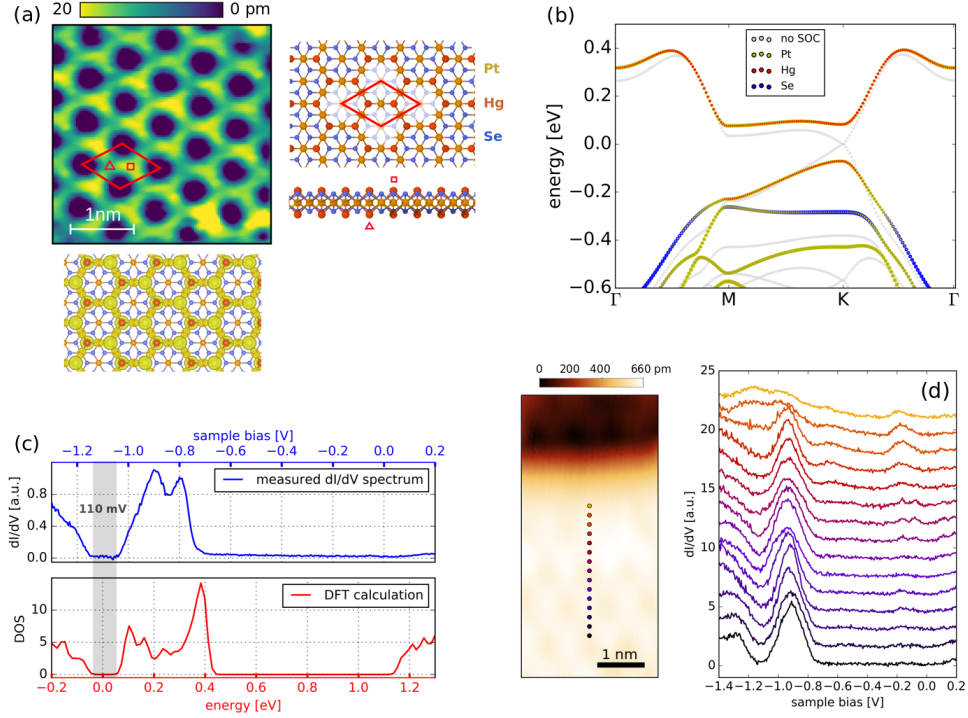


Figure 1: **Atomic and electronic structure of Pt_2HgSe_3 .** (a) Atomic resolution, topographic STM image of Pt_2HgSe_3 , stabilization parameters: 10 pA, -0.8 V. Sublattices are marked with a red triangle and rectangle, respectively. Right inset: atomic structure of Pt_2HgSe_3 , top and side view. Bottom inset: Contour plot of the density of states within the conduction band in a 200 meV interval. (b) Band structure of Pt_2HgSe_3 single layer, from DFT calculation, without (grey) and with (colored) SOC. Size and color of the dots is proportional to the weight of Pt, Hg or Se in the respective electronic state. (c) Comparison of measured $dI/dV(V)$ signal (blue) and calculated (red) density of states. The measurement was conducted on the defect free basal plane of Pt_2HgSe_3 . The calculation is for a monolayer of Pt_2HgSe_3 . Band gap highlighted in gray. (d) Measured dI/dV spectra as a function of distance from a step edge on the basal plane. The spectra are offset for clarity. Topographic STM image of the step shown on the left side of the spectra. The positions of the spectra are shown by dots with the respective colors.

functional theory (DFT) calculations of the monolayer, see red plot in Fig. 1c. The 110 meV gap shown here is a best case scenario, where we purposely selected an area devoid of any surface defects. The large defect concentration of the basal plane (see Supplement S3) makes the local electronic structure inhomogeneous. In order to characterize the gap rigorously, we have measured the band gap from 982 individual spectra in an area $10 \times 10 \text{ nm}^2$. The mean gap value was found to be 78 meV, with a standard deviation of 27 meV (for details see Supplement S4). The topological nature of the band gap is established by calculating the \mathbb{Z}_2 index (see Supplement S7). By comparing the red and blue plots in Fig. 1c, we can immediately see that the calculated LDOS of the monolayer accurately reproduces the dI/dV spectrum measured on the top layer of a bulk crystal. Also considering that the measurement is not reproduced by the calculated surface DOS of a 4 layer slab, suggests that the top Pt_2HgSe_3 layer in our measurement is decoupled from the bulk (see supplement S7.1). This is supported by our STM measurements of the monolayer step height, which is found to be 0.7 \AA larger than the intrinsic interlayer distance of 5.3 \AA (see inset in Fig. 2a and Fig. 1c of the supplement).

Although the measured LDOS is reproduced by the DOS of the monolayer, the sample is heavily n doped. In case of the measured curve in Fig. 1c, the Fermi level marked by zero bias is shifted above the conduction band, leaving the band gap at -1.15 eV . A possible source of the high n doping might be defects or inhomogeneities in the bulk crystal (see Supplement S3). A strong indicator of these is the presence of PtSe_2 in the sample and that in the case of all crystals we observe a large number of adsorbates even on the freshly cleaved basal plane. Investigating the doping in exfoliated crystals down to the bilayer thickness, we find that the n doping is considerably less, with the Fermi level being at least 0.5 V closer to the topological gap than for the bulk (see Supplementary figure 13 and 14). This points to inhomogeneities and defects as being the most likely cause of the doping, as well as the enlarged interlayer spacing.

Having established the location of the band gap in the dI/dV spectra, let us focus on investigating the presence of the predicted QSH edge states³⁶. Other QSH material candidates, such as WTe_2 ²⁹, $\text{Bi}_{14}\text{Rh}_3\text{I}_9$ ³³, and ZrTe_5 ³⁷ also reproduce the LDOS of the monolayer, when measuring the top of bulk crystals with STM. For these materials, monolayer steps on the bulk surface show the hallmark edge states

residing in the band gap. In Fig. 1d, we show individual dI/dV spectra measured near a monolayer step edge on a thick flake, having hundreds of layers. The positions of the spectra are marked by similarly colored dots on the STM image of the step. At a position 2 nm away from the step edge, the spectra reproduce the LDOS measured deep in the bulk of the sample. Moving even closer to the edge, at a distance of ~ 1 nm, the LDOS inside the band gap starts to increase, indicating the presence of an in gap state. An extra state localized to the edge also appears above the conduction band, at -0.2 V, which is a fingerprint of the edge structure. During our STM investigation, straight and atomically clean edges were always of the zigzag kind. Therefore, we checked the atomic and electronic structure of this edge orientation terminated by Se, Pt and Hg, by optimizing the atomic lattice of monolayer ribbons in DFT. The only atomic configuration that shows the hallmark edge state above the conduction band and is energetically stable, is a Se terminated zigzag edge (see Fig. 3 and Supplementary section S8). Thus, we have used this trivial edge state above the conduction band to identify the type of zigzag edge present in the measurement. This allows us to accurately reproduce the LDOS of the edge in our calculations.

In the following we examine in more detail the increased LDOS near the monolayer step edge. In Fig. 2c we show an image of the dI/dV signal at a voltage inside the gap, measured along an edge shown in Fig. 2a. An increased dI/dV signal indicates an increased LDOS near the step. In all panels on Fig. 2 the black dotted lines mark the position of the edge. The decay of the edge state into the bulk is found to be of the order of 5 \AA , in agreement with prediction³⁶. Taking a section between the dotted black lines (Fig. 2d), one observes that the edge LDOS is modulated by the atomic periodicity, as expected for a topological edge state^{20;38}. A further hallmark of topological edge states is that the state is not perturbed by the presence of a defect, visible in the top-right area of Fig. 2a. If backscattering would take place due to the defect this would result in a modulation of the local density of states along the edge. The wavelength of this modulation is determined by the change in crystal momentum of the scattered electron, which can be obtained from the dispersion relation along the edge, shown in Fig. 3a. The voltage used in the measurement (-1.15 V) corresponds to an energy in the middle of the gap. At this energy, the change in crystal momentum would result in a periodicity of 13.1 \AA related to intra-band scattering²⁰. To check the presence of backscattering, we show the Fourier transform of the dI/dV signal

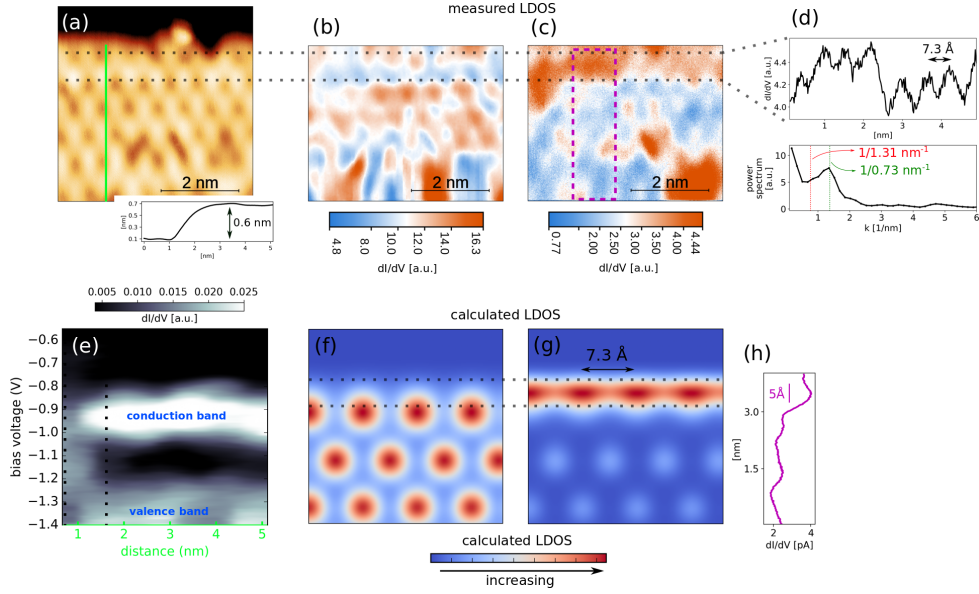


Figure 2: **Characterizing the edge state.** (a) Topographic STM image of a zigzag edge. Stabilization parameters: -0.85 V bias, 30 pA. dI/dV spectra shown in (e) are measured along the green line. Black dotted lines mark the edge, as in (a-c, e-g). Inset: height section of the step. (b) dI/dV image, measured in the same area as the topographic image in (a), outside the gap in the conduction band, at bias voltage -0.85 V. (c) dI/dV image, measured in the same area as (a, b), at a bias voltage of -1.15 V inside the gap. The position of the edge state is marked between two dotted black lines. (d) Top: dI/dV signal modulation along the edge state. Section between the black dotted lines in (c). Bottom: Fast Fourier transform of the line section. (e) Plot of dI/dV spectra measured as a function of distance from the edge. The spectra are recorded along the green line in (c). (f) Calculated LDOS of the conduction band. (g) Calculated LDOS of the edge state, using a broadening of 2.6 Å. LDOS periodicity along the edge is equal to the unit cell size (shown by arrowed black line). Edge state LDOS is concentrated between the dotted black lines. (h) Averaged section across the edge state within the purple dotted box shown in (c). The decay of the edge state into the bulk is of the order of 5 Å, the same as the decay in the calculation: (g) For extended data, see section 10 of the supplement.

along the edge in Fig. 2d. We observe the peak corresponding to $1/0.73 \text{ nm}^{-1}$ unit cell periodicity, but the peak for backscattering is clearly absent. This conclusion is further strengthened by additional Fourier analysis on a longer, irregular edge (see supplement S5). This analysis is essentially a 1D analog of probing the suppression of backscattering on the 2D surface state of strong topological insulators by STM measurement of quasiparticle interference patterns³⁹.

Finally, comparing the dI/dV images with the calculated LDOS map inside the topological gap (Fig. 2g) and of the complete valence band (Fig. 2f), we find that there is good agreement with the measurements. The calculated LDOS maps reproduce both the atomic periodicity along the edge state, as well as its decay length of 5 \AA . With such a small decay length, it is expected that the edge state would start to develop at defect sites inside the basal plane, such as in the bottom-right corner of Fig. 2c. A better example of this effect can be observed in the supplementary Fig. 4d.

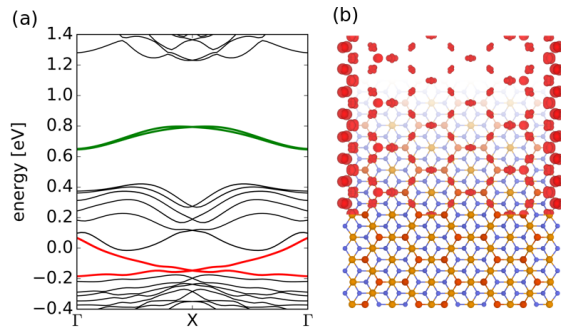


Figure 3: **Pt₂HgSe₃ nanoribbon. Topological edge states.** (a) Band structure of a 3.2 nm wide zigzag ribbon, calculated using DFT. Topological edge state is shown in red, while the trivial edge state above the conduction band is shown in green. (b) LDOS contour plot of the topological edge state integrated over the whole topological band.

The relatively weak van der Waals bond between the monolayers of Pt₂HgSe₃ makes it possible to exfoliate the material, potentially to the monolayer limit⁶. We demonstrated this possibility by using the standard "scotch tape method" to exfoliate thin flakes onto a SiO₂ substrate or a polymer stack, as used in dry stacking of 2D materials⁴⁰ (see Fig. 4a-c). Using dry stacking, it should be possible to place Pt₂HgSe₃ on the surface of a high T_c superconductor, enabling the investigation of high temperature Majorana zero modes⁹. The thinnest crystals we were able to prepare by

conventional scotch tape exfoliation onto SiO_2 substrates was 5 layers. However, these crystals have lateral sizes below $1\ \mu\text{m}$ (see Fig. 4c), severely limiting their usefulness. Exfoliating onto fresh gold surfaces⁴¹ increases the lateral size of the flakes significantly and their thickness, measured by AFM is $1.3\ \text{nm}$ (see Fig. 4d, e). However, these thin flakes are found to be highly disordered. For more details see supplementary section S9. These results show that it should be possible to exfoliate single layers of Pt_2HgSe_3 onto SiO_2 and especially gold substrates, but the material homogeneity and defect density of the bulk crystals needs to be improved significantly. Further improvements in crystal quality could also be a key to probing the dual topological nature^{42;43} of Pt_2HgSe_3 such as in the case of Bi_2TeI ⁴⁴. This is because Pt_2HgSe_3 is predicted to not only be the long sought after Kane-Mele insulator, but in it's bulk form it is also a topological crystalline insulator and a \mathbb{Z}_2 insulator^{42;43;45}.

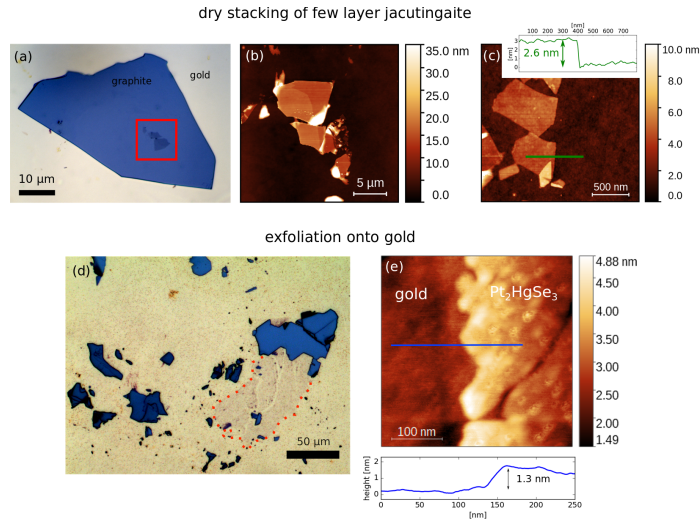


Figure 4: **Exfoliation of Pt_2HgSe_3 .** (a) Stack of jacutingaite on graphite, prepared by dry stacking. (b) AFM image of the flake before the transfer supported on a PMMA substrate. (c) AFM image of a thin flake, having a thickness of $2.6\ \text{nm}$, corresponding to approximately 5 single layers. Inset: height section of the flake along the green line. (d) Exfoliation of jacutingaite onto a gold (111) surface. The thinnest flakes are marked by the red dotted line. (e) AFM image of the thinnest flakes, inside the area marked with red in (d). Inset: height section along the blue line.

One of the most promising QSH materials is monolayer $1\text{T}'\text{-WTe}_2$, but the chemical stability of Pt_2HgSe_3 in air and it's band gap above room temperature, clearly

sets it aside. The main difference being that WTe_2 rapidly oxidizes under ambient conditions and shows the QSH effect only below a temperature of 100 K³⁰. Our results establish that jacutingaite is a new and widely accessible platform to explore the properties of helical one dimensional electron systems^{20;46} and should be available for charge transport measurements, even in the monolayer, if the defect concentration and sample homogeneity can be improved. Recent theoretical studies highlight the possibility of superconductivity in doped Pt_2HgSe_3 ⁴⁷, this could open a way to explore the coexistence of topological edge states in proximity to a superconductor in the same material system. Additionally, a non zero \mathbb{Z}_4 index⁴⁸ makes Pt_2HgSe_3 a fertile playground to explore higher order topology. In our samples the Fermi level is already shifted above the type-II van Hove singularity where superconductivity is expected, possibly due to the presence of lattice defects. Our results hint at the possibility that tuning the composition, may be an effective tool to control the doping of Pt_2HgSe_3 , similarly to quaternary topological insulators⁴⁹.

Data availability

The datasets generated during and/or analysed during the current study are available from the corresponding author on reasonable request.

Acknowledgments

L.T. acknowledges financial support from the ERC Starting grant NanoFab2D. P.N.I. acknowledges support from the Hungarian Academy of Sciences, Lendület Program, grant no: LP2017-9/2017. The work was conducted within the Graphene Flagship, H2020 Graphene Core2 project no. 785219 and the Quantum Technology National Excellence Program (Project No. 2017-1.2.1-NKP-2017-00001). Work was supported by the National Research, Development and Innovation Office (Hungary) grant No. FK 125063 (Á.P., Ka.K.), K-115608 (J.K. and G.K.), KH130413 (V.P.) and K108753 (L.T.). J.K. and G.K. acknowledge the ELTE Excellence Program (1783-3/2018/FEKUTSTRAT) supported by the Hungarian Ministry of Human Capacities. V.P. acknowledges the Janos Bolyai Research Scholarship of the Hungarian Academy of Sciences. J.K. was supported by the UNKP-19-4 New National Excellence Program of the Ministry for Innovation and Technology. A.V. acknowledges financial

support from the Grant Agency of the Czech Republic (project No. 18-15390S). We acknowledge NIIF for awarding us access to computing resources based in Hungary at Debrecen. Ka.K. acknowledges grant no. VEKOP-2.3.2-16-2016-00011.

Associated Content

The Supporting Information is available free of charge on the ACS Publications website at DOI: ...

Supplementary sections 1 to 9: Detailing the sample preparation and STM measurement, additional information on defects, band gap statistics, measurements on irregular, monolayer edges, Raman measurements, density functional theory calculation details, various edge configurations, details on exfoliation.

Author contributions

Ko.K. did the exfoliation experiments and STM measurements, with the supervision of P.N-I. Á.H. helped with sample preparation. A.V. provided the sample. P.V., G.K. and J.K. performed the DFT calculations. G.B., Á.P. and Ka.K. performed the Raman measurements, while G.K. calculated the Raman spectrum, under the supervision of J.K. A.V. and Z.E.H. performed the XRD measurement. P.N-I. conceived the project and coordinated it together with L.T. P.N-I. wrote the manuscript, with contributions from all authors.

References

- [1] Joel E Moore. The birth of topological insulators. *Nature*, 464(7286):194–198, mar 2010.
- [2] M. Hasan and C. Kane. Colloquium: Topological insulators. *Rev. Mod. Phys.*, 82(4):3045–3067, nov 2010.
- [3] M. Konig, Steffen Wiedmann, C. Brune, Andreas Roth, Hartmut Buhmann, Laurens W Molenkamp, X.-L. Qi, and S.-C. Zhang. Quantum Spin Hall Insulator State in HgTe Quantum Wells. *Science*, 318(5851):766–770, nov 2007.
- [4] C. L. Kane and E. J. Mele. Quantum Spin Hall Effect in Graphene. *Phys. Rev. Lett.*, 95(22):226801, nov 2005.
- [5] C. L. Kane and E. J. Mele. Z(2) Topological Order and the Quantum Spin Hall Effect. *Phys. Rev. Lett.*, 95(14):146802, sep 2005.
- [6] Nicolas Mounet, Marco Gibertini, Philippe Schwaller, Davide Campi, Andrius Merkys, Antimo Marrazzo, Thibault Sohier, Ivano Eligio Castelli, Andrea Cepellotti, Giovanni Pizzi, and Nicola Marzari. Two-dimensional materials from high-throughput computational exfoliation of experimentally known compounds. *Nat. Nanotechnol.*, 13(3):246–252, mar 2018.
- [7] Justin C. W. Song and Nathaniel M. Gabor. Electron quantum metamaterials in van der Waals heterostructures. *Nat. Nanotechnol.*, 13(11):986–993, nov 2018.
- [8] A. K. Geim and I. V. Grigorieva. Van der Waals heterostructures. *Nature*, 499(7459):419–425, jul 2013.
- [9] Zhongbo Yan, Fei Song, and Zhong Wang. Majorana Corner Modes in a High-Temperature Platform. *Phys. Rev. Lett.*, 121(9):096803, aug 2018.
- [10] Liangzhi Kou, Binghai Yan, Feiming Hu, Shu-Chun Wu, Tim O. Wehling, Claudia Felser, Changfeng Chen, and Thomas Frauenheim. Graphene-Based Topological Insulator with an Intrinsic Bulk Band Gap above Room Temperature. *Nano Lett.*, 13(12):6251–6255, dec 2013.

- [11] Liangzhi Kou, Shu-chun Wu, Claudia Felser, Thomas Frauenheim, Changfeng Chen, and Binghai Yan. Robust 2D Topological Insulators in van der Waals Heterostructures. *ACS Nano*, 8(10):10448–10454, oct 2014.
- [12] Abdulrhman M. Alsharari, Mahmoud M Asmar, and Sergio E Ulloa. Mass inversion in graphene by proximity to dichalcogenide monolayer. *Phys. Rev. B*, 94(24):241106, dec 2016.
- [13] Jayakumar Balakrishnan, Gavin Kok Wai Koon, Manu Jaiswal, a. H. Castro Neto, and Barbaros Özyilmaz. Colossal enhancement of spin–orbit coupling in weakly hydrogenated graphene. *Nat. Phys.*, 9(4):284–287, mar 2013.
- [14] T. Namba, K. Tamura, K. Hatsuda, T. Nakamura, C. Ohata, S. Katsumoto, and J. Haruyama. Spin–orbit interaction in Pt or Bi₂Te₃ nanoparticle-decorated graphene realized by a nanoneedle method. *Appl. Phys. Lett.*, 113(5):053106, jul 2018.
- [15] A. Avsar, J. Y. Tan, T. Taychatanapat, J. Balakrishnan, G.K.W. Koon, Y. Yeo, J. Lahiri, A. Carvalho, a. S. Rodin, E.C.T. O’Farrell, G. Eda, a. H. Castro Neto, and B. Özyilmaz. Spin–orbit proximity effect in graphene. *Nat. Commun.*, 5:4875, sep 2014.
- [16] Zhe Wang, Dong–Keun Ki, Hua Chen, Helmuth Berger, Allan H. MacDonald, and Alberto F. Morpurgo. Strong interface-induced spin–orbit interaction in graphene on WS₂. *Nat. Commun.*, 6:8339, sep 2015.
- [17] Zhe Wang, Dong-keun Ki, Jun Yong Khoo, Diego Mauro, Helmuth Berger, Leonid S Levitov, and Alberto F Morpurgo. Origin and Magnitude of ‘Designer’ Spin-Orbit Interaction in Graphene on Semiconducting Transition Metal Dichalcogenides. *Phys. Rev. X*, 6(4):041020, oct 2016.
- [18] Yafei Ren, Zhenhua Qiao, and Qian Niu. Topological phases in two-dimensional materials: a review. *Reports Prog. Phys.*, 79(6):066501, jun 2016.
- [19] F. Reis, G. Li, L. Dudy, M. Bauernfeind, S. Glass, W. Hanke, R. Thomale, J. Schäfer, and R. Claessen. Bismuthene on a SiC substrate: A candidate for a high-temperature quantum spin Hall material. *Science*, 357(6348):287–290, jul 2017.

- [20] R. Stühler, F. Reis, T. Müller, T. Helbig, T. Schwemmer, R. Thomale, J. Schäfer, and R. Claessen. Tomonaga–Luttinger liquid in the edge channels of a quantum spin Hall insulator. *Nat. Phys.*, 16(1):47–51, jan 2020.
- [21] Jialiang Deng, Bingyu Xia, Xiaochuan Ma, Haoqi Chen, Huan Shan, Xiaofang Zhai, Bin Li, Aidi Zhao, Yong Xu, Wenhui Duan, Shou-Cheng Zhang, Bing Wang, and J. G. Hou. Epitaxial growth of ultraflat stanene with topological band inversion. *Nat. Mater.*, 17(12):1081–1086, dec 2018.
- [22] Ilya K. Drozdov, A. Alexandradinata, Sangjun Jeon, Stevan Nadj-Perge, Huiwen Ji, R. J. Cava, B. Andrei Bernevig, and Ali Yazdani. One-dimensional topological edge states of bismuth bilayers. *Nat. Phys.*, 10(9):664–669, aug 2014.
- [23] Lang Peng, Jing-Jing Xian, Peizhe Tang, Angel Rubio, Shou-Cheng Zhang, Wenhao Zhang, and Ying-Shuang Fu. Visualizing topological edge states of single and double bilayer Bi supported on multibilayer Bi(111) films. *Phys. Rev. B*, 98(24):245108, dec 2018.
- [24] X. Qian, J. Liu, L. Fu, and J. Li. Quantum spin Hall effect in two-dimensional transition metal dichalcogenides. *Science*, 346(6215):1344–1347, dec 2014.
- [25] Hai Xu, Dong Han, Yang Bao, Fang Cheng, Zijing Ding, Sherman J. R. Tan, and Kian Ping Loh. Observation of Gap Opening in 1T' Phase MoS₂ Nanocrystals. *Nano Lett.*, 18(8):5085–5090, aug 2018.
- [26] P. Chen, Woei Wu Pai, Y.-H. Chan, W.-L. Sun, C.-Z. Xu, D.-S. Lin, M. Y. Chou, A.-V. Fedorov, and T.-C. Chiang. Large quantum-spin-Hall gap in single-layer 1T' WSe₂. *Nat. Commun.*, 9(1):2003, dec 2018.
- [27] Miguel M Ugeda, Artem Pulkin, Shujie Tang, Hyejin Ryu, Quansheng Wu, Yi Zhang, Dillon Wong, Zahra Pedramrazi, Ana Martín-Recio, Yi Chen, Feng Wang, Zhi-Xun Shen, Sung-Kwan Mo, Oleg V. Yazyev, and Michael F. Crommie. Observation of topologically protected states at crystalline phase boundaries in single-layer WSe₂. *Nat. Commun.*, 9(1):3401, dec 2018.
- [28] Shujie Tang, Chaofan Zhang, Dillon Wong, Zahra Pedramrazi, Hsin-zon Tsai, Chunjing Jia, Brian Moritz, Martin Claassen, Hyejin Ryu, Salman Kahn, Juan Jiang, Hao Yan, Makoto Hashimoto, Donghui Lu, Robert G Moore, Chan-Cuk

- Hwang, Choongyu Hwang, Zahid Hussain, Yulin Chen, Miguel M Ugeda, Zhi Liu, Xiaoming Xie, Thomas P Devereaux, Michael F Crommie, Sung-kwan Mo, and Zhi-xun Shen. Quantum spin Hall state in monolayer 1T'-WTe₂. *Nat. Phys.*, 13(7):683–687, jun 2017.
- [29] Lang Peng, Yuan Yuan, Gang Li, Xing Yang, Jing-jing Xian, Chang-jiang Yi, You-Guo Shi, and Ying-shuang Fu. Observation of topological states residing at step edges of WTe₂. *Nat. Commun.*, 8(1):659, dec 2017.
- [30] Sanfeng Wu, Valla Fatemi, Quinn D Gibson, Kenji Watanabe, Takashi Taniguchi, Robert J Cava, and Pablo Jarillo-Herrero. Observation of the quantum spin Hall effect up to 100 kelvin in a monolayer crystal. *Science*, 359(6371):76–79, jan 2018.
- [31] Wang Chen, Xuedong Xie, Junyu Zong, Tong Chen, Dongjin Lin, Fan Yu, Shaoen Jin, Lingjie Zhou, Jingyi Zou, Jian Sun, Xiaoxiang Xi, and Yi Zhang. Growth and Thermo-driven Crystalline Phase Transition of Metastable Monolayer 1T'-WSe₂ Thin Film. *Sci. Rep.*, 9(1):2685, dec 2019.
- [32] Bertold Rasche, Anna Isaeva, Alexander Gerisch, Martin Kaiser, Wouter Van den Broek, Christoph T. Koch, Ute Kaiser, and Michael Ruck. Crystal Growth and Real Structure Effects of the First Weak 3D Stacked Topological Insulator Bi₁₄Rh₃I₉. *Chem. Mater.*, 25(11):2359–2364, jun 2013.
- [33] Christian Pauly, Bertold Rasche, Klaus Koepf, Manuel Richter, Sergey Borisenko, Marcus Liebmann, Michael Ruck, Jeroen van den Brink, and Markus Morgenstern. Electronic Structure of the Dark Surface of the Weak Topological Insulator Bi₁₄Rh₃I₉. *ACS Nano*, 10(4):3995–4003, apr 2016.
- [34] A. R. Cabral, H. F. Galbiatti, R. Kwitko-Ribeiro, and B. Lehmann. Platinum enrichment at low temperatures and related microstructures, with examples of hongshiite (PtCu) and empirical 'Pt₂HgSe₃' from Itabira, Minas Gerais, Brazil. *Terra Nov.*, 20(1):32–37, jan 2008.
- [35] Anna Vymazalova, Frantisek Laufek, Milan Drabek, Alexandre Raphael Cabral, Jakub Haloda, Tamara Sidorinova, Bernd Lehmann, Henry Francisco Galbiatti, and Jan Drahokoupil. Jacutingaite, Pt₂HgSe₃, a new platinum-group mineral

- species from the caue iron-ore deposit, Itabira District, Minars-Gerais, Brazil. *Can. Mineral.*, 50(2):431–440, apr 2012.
- [36] Antimo Marrazzo, Marco Gibertini, Davide Campi, Nicolas Mounet, and Nicola Marzari. Prediction of a Large-Gap and Switchable Kane-Mele Quantum Spin Hall Insulator. *Phys. Rev. Lett.*, 120(11):117701, mar 2018.
- [37] R Wu, J.-Z. Ma, S.-M. Nie, L.-X. Zhao, X Huang, J.-X. Yin, B.-B. Fu, P. Richard, G.-F. Chen, Z. Fang, X. Dai, H.-M. Weng, T. Qian, H. Ding, and S. H. Pan. Evidence for Topological Edge States in a Large Energy Gap near the Step Edges on the Surface of ZrTe5. *Phys. Rev. X*, 6(2):021017, may 2016.
- [38] Christian Pauly, Bertold Rasche, Klaus Koepernik, Marcus Liebmann, Marco Prutzer, Manuel Richter, Jens Kellner, Markus Eschbach, Bernhard Kaufmann, Lukasz Plucinski, Claus M. Schneider, Michael Ruck, Jeroen van den Brink, and Markus Morgenstern. Subnanometre-wide electron channels protected by topology. *Nat. Phys.*, 11(4):338–343, mar 2015.
- [39] Pedram Roushan, Jungpil Seo, Colin V. Parker, Y. S. Hor, D. Hsieh, Dong Qian, Anthony Richardella, M. Z. Hasan, R. J. Cava, and Ali Yazdani. Topological surface states protected from backscattering by chiral spin texture. *Nature*, 460(7259):1106–1109, aug 2009.
- [40] Filippo Pizzocchero, Lene Gammelgaard, Bjarke S. Jessen, José M. Caridad, Lei Wang, James Hone, Peter Bøggild, and Timothy J. Booth. The hot pick-up technique for batch assembly of van der Waals heterostructures. *Nat. Commun.*, 7(May):11894, jun 2016.
- [41] Gábor Zsolt Magda, János Pető, Gergely Dobrik, Chanyong Hwang, László P. Biró, and Levente Tapasztó. Exfoliation of large-area transition metal chalcogenide single layers. *Sci. Rep.*, 5:14714, oct 2015.
- [42] Jorge I. Facio, Sanjib Kumar Das, Yang Zhang, Klaus Koepernik, Jeroen van den Brink, and Ion Cosma Fulga. Dual topology in jacutingaite Pt₂HgSe₃. *Phys. Rev. Mater.*, 3(7):074202, jul 2019.
- [43] Antimo Marrazzo, Nicola Marzari, and Marco Gibertini. Emergent dual topology

- in the three-dimensional Kane-Mele Pt₂HgSe₃. *Phys. Rev. Res.*, 2(1):012063, mar 2020.
- [44] Nurit Avraham, Abhay Kumar Nayak, Aviram Steinbok, Andrew Norris, Huixia Fu, Yan Sun, Yanpeng Qi, Lin Pan, Anna Isaeva, Alexander Zeugner, Claudia Felser, Binghai Yan, and Haim Beidenkopf. Visualizing coexisting surface states in the weak and crystalline topological insulator Bi₂TeI. *Nat. Mater.*, 19(6):610–616, jun 2020.
- [45] I. Cucchi, A. Marrazzo, E. Cappelli, S. Riccò, F. Y. Bruno, S Lisi, M Hoesch, T. K. Kim, C. Cacho, C. Besnard, E. Giannini, N. Marzari, M. Gibertini, F. Baumberger, and A. Tamai. Bulk and Surface Electronic Structure of the Dual-Topology Semimetal Pt₂HgSe₃. *Phys. Rev. Lett.*, 124(10):106402, mar 2020.
- [46] Pietro Novelli, Fabio Taddei, Andre K. Geim, and Marco Polini. Failure of Conductance Quantization in Two-Dimensional Topological Insulators due to Nonmagnetic Impurities. *Phys. Rev. Lett.*, 122(1):016601, jan 2019.
- [47] Xianxin Wu, Mario Fink, Werner Hanke, Ronny Thomale, and Domenico Di Sante. Unconventional superconductivity in a doped quantum spin Hall insulator. *Phys. Rev. B*, 100(4):041117, jul 2019.
- [48] M G Vergniory, L Elcoro, Claudia Felser, Nicolas Regnault, B Andrei Bernevig, and Zhijun Wang. A complete catalogue of high-quality topological materials. *Nature*, 566(7745):480–485, feb 2019.
- [49] T. Arakane, T. Sato, S. Souma, K. Kosaka, K. Nakayama, M. Komatsu, T. Takahashi, Zhi Ren, Kouji Segawa, and Yoichi Ando. Tunable Dirac cone in the topological insulator Bi_{2-x}Sb_xTe_{3-y}Se_y. *Nat. Commun.*, 3(1):636, jan 2012.